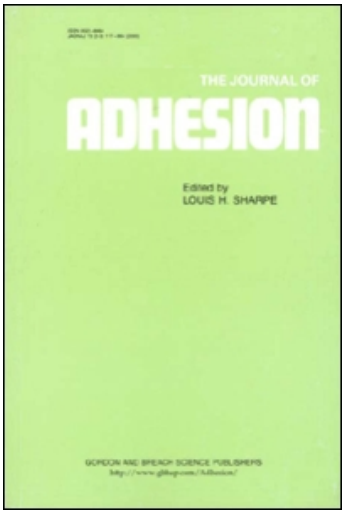

The Journal of Adhesion
Publication details, including instructions for authors and subscription information:
http://www.informaworld.com/smpp/title~content=t713453635

Deformation mechanisms at the interface between grafted polyethylene and ethylene/vinyl alcohol copolymer

Antoine Guiu[a]; Martin E. R. Shanahan[a]
[a] Centre des Matériaux de Grande Diffusion Ecole des Mines d'AlésAles Cedex, France

Online publication date: 08 September 2010

To cite this Article Guiu, Antoine and Shanahan, Martin E. R.(2003) 'Deformation mechanisms at the interface between grafted polyethylene and ethylene/vinyl alcohol copolymer', The Journal of Adhesion, 79: 5, 419 — 442
To link to this Article: DOI: 10.1080/00218460309563
URL: http://dx.doi.org/10.1080/00218460309563

The Journal of Adhesion, 79: 419–442, 2003

0021-8464/03 $12.00 +.00
DOI: 10.1080/00218460390214217

Taylor & Francis
Taylor & Francis Group

DEFORMATION MECHANISMS AT THE INTERFACE BETWEEN GRAFTED POLYETHYLENE AND ETHYLENE/VINYL ALCOHOL COPOLYMER

Antoine Guiu
Martin E. R. Shanahan
Centre des Matériaux de Grande Diffusion
Ecole des Mines d'Alés
Ales Cedex, France

The adhesion of grafted polyethylene (PEg) to an ethylene/vinyl alcohol copolymer (EVOH), has been studied using different peel configurations and angles. Overall peel energies have been obtained and found to depend on peel angle. Experimental and theoretical studies of local peel arm curvature and opening angles near the crack front led to good agreement, the latter being based on elastic foundation theory and global elasto-plastic analysis. Having established the validity of the analysis used, the contribution to the peel energy pertaining to bulk bending of the peel arm(s) was estimated, allowing the local adhesion energy to be isolated. This was found to be virtually independent of peel angle. Scanning electron microscopy examination revealed a plastic, fibrillar craze zone in the PEg corresponding to a Dugdale zone. Nevertheless, adhesion energy was higher than expected from the Dugdale model. Energy dissipation in the vicinity of the Dugdale zone associated with shear deformation, and thus without apparent cavitation, may contribute to fracture energy. A rough estimate of the energy expended during the observed change in orientation of fibrils in the relaxation zone after the crack tip shows this contribution to be significant.

Keywords: Adhesion; Crazing; Energy dissipation; Ethylene/vinyl alcohol copolymer; Grafting; Peel; Polyethylene; Shear

Received 8 February 2002; in final form 23 September 2002.

The authors are indebted to Atofina for financial and material support, and to members of their research staff for enthusiastic discussions.

Address correspondence to Professor Martin E. R. Shanahan, Centre des Matériaux de Grande Diffusion, Ecole des Mines d'Alès, 6, Avenue de Clavières, 30319 Ales Cedex, France. E-mail: martin.shanahan@ema.fr

INTRODUCTION

Various adhesion mechanisms may come into play between two polymers in contact. These will depend on the nature of the polymers in question, but also on conditions of assembly (temperature, time, pressure) and subsequent circumstances. For mutually compatible polymers, macromolecular chain diffusion is often a major mechanism, especially if assembly involves elevated temperatures [1, 2] Similar interfacial strength may be expected when chemical bonding occurs [3] and even wetting/adsorption (van der Waals) interactions can lead to good practical adhesion [4].

The peel test is one of the most frequently used tests for measuring the strength of polymeric laminate interfaces. However, it has been well established, since the early work of Gent and Petrich [5] that bulk energy losses due to deformation of the peel arm(s) can markedly increase effective adhesive strength. Various types of deformation may intervene but, in the present contribution, we are principally concerned with dissipation due to bending, since the high tensile resistance of the system studied renders plastic deformation in tension negligible. Methods to assess the energy dissipated in bending the peel arm have been applied, based on an elastoplastic analysis of the arm and an estimate of the curvature of the beam at the crack tip. This curvature may be monitored either by forcing the beam to curve around rollers of known curvature [6, 7] or by measuring the effective curvature during the test [8, 9]. Development of the global and local analysis of beam deformation [10, 11] has led to a model, proposed by Williams and Kinloch [12, 13] to estimate local parameters such as the curvature, k_0, and the opening angle, θ_0, of the beam arm at the crack tip. This model is based on global, elastoplastic analysis and local, beam on elastic foundation theory [14, 15]. Good agreement was obtained between calculated and experimental values for L-type peeling of polymeric laminates on rigid substrates. However, to our knowledge, no studies of T-type peeling, or very strong interfaces, where peel energies are over 10 $kJ \cdot m^{-2}$, have been reported in the literature. Beam on an elastic foundation theory may also be applied to estimate local stresses near crack tip [14, 16].

Failure mechanisms of polymer interfaces reinforced with block copolymers have been widely studied for amorphous polymers but only recently for semicrystalline polymers. In the case of amorphous polymers, it has been shown that, for sufficiently strong interfaces, plastic deformation mechanisms are activated in the adhesive, near the interface [17]. Recent microscopic studies have revealed that crazing is the main mechanism of deformation during fracture of amorphous

polymer interfaces [18], as well as for semicrystalline interfaces [19]. When a well-defined craze propagates ahead of the crack tip, the Dugdale [20] model can be used to give an estimate of the energy, G, dissipated in the plastic zone [21] such that, in the framework of linear elastic fracture mechanics [LEFM],

$$G = \int_0^{\delta_c} \sigma(\delta) \mathrm{d}\delta = \int_0^{\delta_c} \sigma_0 \, \mathrm{d}\delta = \sigma_0 \delta_c, \tag{1}$$

where δ and δ_c are, respectively, crack-opening displacement (COD) and its critical value at the transition between the cohesive zone and the void and σ_0 is the stress at the craze/bulk interface, which is assumed to be constant. Craze regions observed both in amorphous polymers such as poly(methyl methocrylate) (PMMA) [22] and in semicrystalline polymers [9, 23] appear to correspond to Dugdale zones [21, 24] and the Dugdale model may apply for amorphous [18] as well as semi-crystalline materials [23]. However, in recent work on the adhesion of two semicrystalline polymers, two interesting findings were obtained. Firstly, the calculated value of local fracture energy, G_A, exceeded expectations pertaining to Equation (1). Secondly, observation of peel fracture fronts revealed that the energy dissipation mechanisms had not ceased abruptly at the transition between cohesive zone and void (at δ_c).

In the following, we have studied a system composed of high density polyethylene, constituting a relatively mechanically resistant material, bonded to a polymer resistant to organic solvents, using an "adhesive" layer, based on maleic-anhydride-grafted polyethylene. This type of multilayer system is now widely used for various industrial applications to give better mechanical, as well as fluid-proof, performance than homogeneous materials. Adhesion between adhesive and barrier material is assured by an *in situ* copolymer formation between maleic anhydride and the barrier polymer. The aim of this work is to study the validity of the model developed to calculate the energy dissipated in bending during peel, and to estimate the local energy responsible for the adhesion. A study of deformation mechanisms at the interface is based on local stress analysis and micrographs of the peel front.

THEORY

Let us consider the L-peel of a beam of width b at an angle θ from a rigid substrate, as shown in Figure 1 (the term "L-peel" refers to the test appearance for $\theta = 90^\circ$). For $x > 0$, the beam is in contact, via an

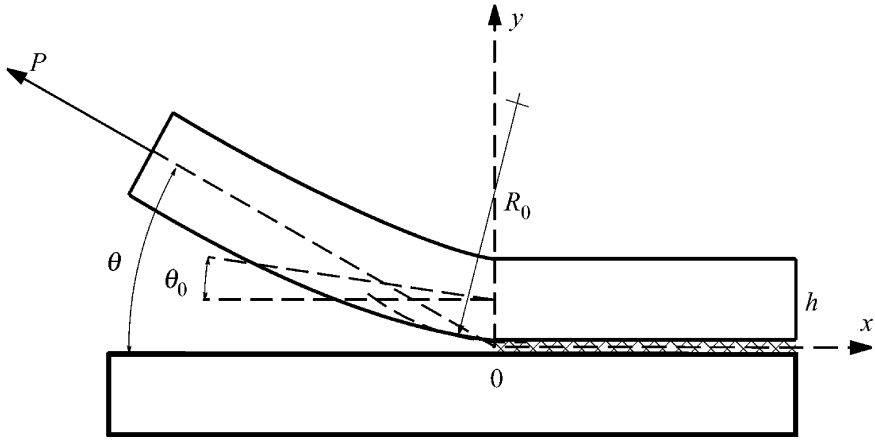

FIGURE 1 L-peel test and notations.

adhesive layer, with the rigid substrate. For $x < 0$, the beam is peeled, and a force P is applied at its extremity. At $x = 0$, the beam adopts a local radius of curvature, R_0, and an opening angle, θ_0, may be observed. The peel energy, G_P, required in the separation of the beam from the substrate is, provided peel arm extension is negligible,

$$G_P = \frac{P}{b}(1 - \cos\theta). \tag{2}$$

In a recent paper [9], we studied the effect of peel geometry on effective peel energy. We developed a mechanical analysis of the peel test, based on perfect elastoplastic behaviour of the material, from which we were able to calculate the energy, G_F, dissipated by flexion of the beam, from the actual curvature, k_0, of the beam at the crack tip:

$$G_F = \frac{h\sigma_0^2}{2E} f_1(k_0), \tag{3}$$

where h, E, σ_0 are, respectively, the thickness, Young's modulus, and yield stress of the beam and k_0 is the relative curvature, defined as the ratio of the radius $R_e = hE/2\sigma_0$ at which the outer fibre of the beam reaches its elastic limit, to the actual radius of curvature, R_0, such that

$$k_0 = \frac{hE}{2\sigma_0}\frac{1}{R_0}. \tag{4}$$

$f_1(k_0)$ is a function of the local curvature, k_0, which may be found in the literature for perfect elastoplastic behaviour of the beam [9, 11, 12]

for bilinear elastoplastic behaviour [13, 25] and for power-law elastoplastic behaviour [10].

We were then able to estimate the intrinsic energy of adhesion, G_A, from the global energy balance equation:

$$G_A = \frac{P}{b}(1 - \cos\theta) - G_F. \tag{5}$$

Note that in Equation (5), the elastic term, introduced by Kendall [26], has been neglected in comparison with the dissipated energy. To estimate G_F, it is possible [8, 9, 27], although relatively inaccurate, to measure the radius of curvature, R_0, of the beam close to the crack tip and deduce the curvature, k_0, from Equation (4).

However, recent theoretical investigations [10–13] of the peel test allow us to calculate the curvature, k_0. The model is based on two equations, one issuing from local analysis of the unpeeled part of the beam, and the other from global analysis of the peeled part of the beam.

Local Analysis

The theory of a beam on an elastic foundation [15, 28] may be applied to the unpeeled part of the beam ($x > 0$) [12, 14, 16]. If we assume small and elastic displacements in the unpeeled part, the general displacement of the neutral surface of the beam under load may be written as [15]

$$y(x) = \mathrm{e}^{-\lambda x}(A\cos\lambda x + B\sin\lambda x), \tag{6}$$

where λ, A, and B are constants. When the beam is composite, with one material of Young's modulus, E, and thickness, h, and the second a thin adhesive of Young's modulus, E_a, and thickness, $h_a \ll h, \lambda$, may be written [14, 29]

$$\lambda = \frac{6^{1/4}}{h}\left(1 + 2\frac{Eh_a}{E_a h}\right)^{-1/4}. \tag{7}$$

Applying boundary conditions at $x = 0$ (since $y'(0) \approx 0$, and $y'''(x) = \frac{\mathrm{d}y''(x)}{\mathrm{d}x} \approx \frac{1}{EI}\frac{\mathrm{d}M}{\mathrm{d}x}$, where $I = bh^3/12$ and M is bending moment):

$$\begin{aligned} y''(0) &= \frac{1}{R_0}, \\ y'''(0) &= \frac{P\sin(\theta - \theta_0)}{EI}, \end{aligned} \tag{8}$$

we get

$$y(x) = \frac{1}{2\lambda^2 R_0} e^{-\lambda x} \left[\left(1 + \frac{R_0}{EI} \frac{P \sin(\theta - \theta_0)}{\lambda} \right) \cos \lambda x - \sin \lambda x \right], \; x \geq 0. \quad (9)$$

The root rotation angle, θ_0, is described by the implicit equation:

$$\theta_0 = \frac{1}{\lambda R_0} + \frac{P \sin(\theta - \theta_0)}{2EI\lambda^2}, \quad (10)$$

and the global displacement of the (neutral surface of the) beam at crack tip, y_0, is

$$y(0) = \frac{1}{2\lambda^2 R_0} \left(1 + \frac{R_0 P \sin(\theta - \theta_0)}{EI\lambda} \right). \quad (11)$$

Global Analysis

An elastoplastic analysis, based on local force and moment equilibrium of the peeled part of the beam ($x < 0$), and taking into account the root rotation angle, θ_0 [10, 13], leads to an expression linking macroscopic parameters (P, θ) to local parameters (k_0, θ_0), *via*

$$\frac{h\sigma_0^2}{2E} f_2(k_0) = \frac{P}{b} [1 - \cos(\theta - \theta_0)], \quad (12)$$

where $f_2(k_0)$ is a function depending only on the local curvature, k_0.

Here again, expressions for $f_2(k_0)$ for various types of material behaviour may be found in the literature [9–13, 25]. Solving Equations (10) and (12) numerically, one can find θ_0 and k_0, and then deduce G_F from Equation (3) and G_A from Equation (5).

The analysis presented here has previously been applied to L-type peel tests, and good agreement was found between experimental and theoretical values of opening angles [12, 13, 30]. However, with small arrangements, this analysis may also be applied to T-peel tests. For T-peel tests, both arms are bent, and a natural angle, θ, may be observed between the direction of the applied force and the plane of the unpeeled part of the specimen (Figure 2). We then have to define four geometrical parameters instead of two, relating to both arms: θ_{01}, θ_{02}, k_{01}, k_{02}, where the additional subscripts 1 and 2 refer to the two arms. A system of four equations equivalent to Equations (10) and (12) can then be found. We then calculate the curvatures k_{01} and k_{02}, estimate the global energy dissipated in bending for the two arms $G_F = G_{F1} + G_{F2}$ from Equation (3), and finally deduce G_A from Equation (5).

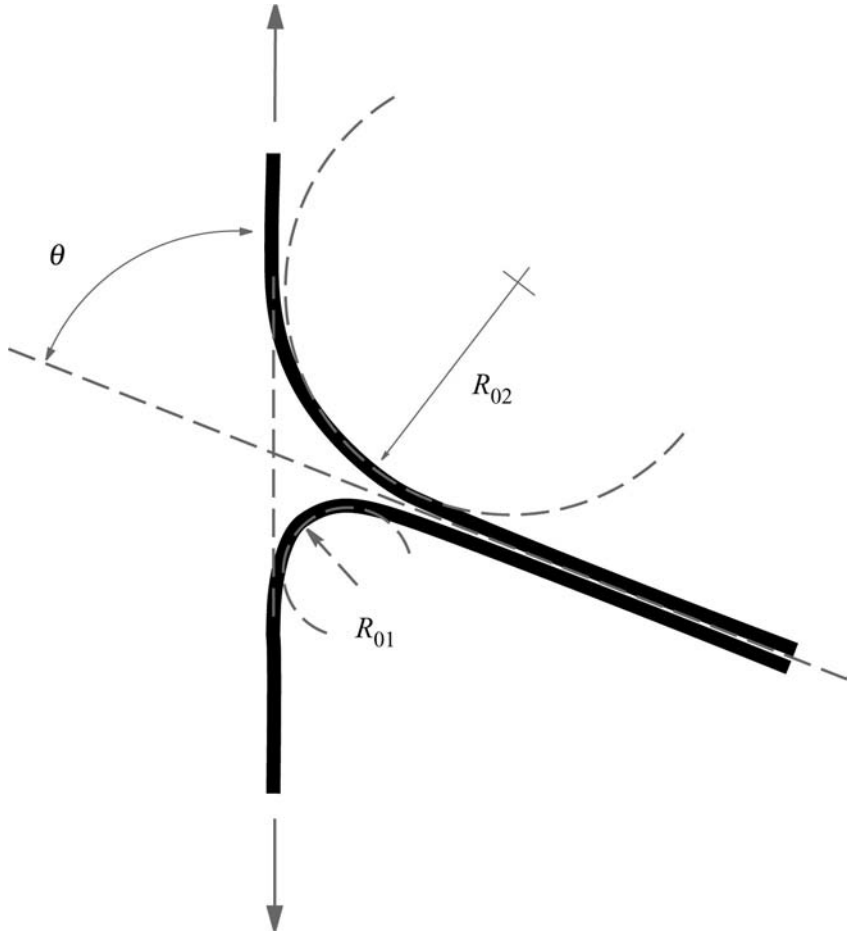

FIGURE 2 T-peel test and notations.

EXPERIMENTAL

Materials

The system studied corresponds to a five-layer polymer system formed by coextrusion and blow-moulding at 230°C. Two outer layers are in high-density polyethylene (HDPE) of *ca.* 1.2 mm thickness each, and a central "barrier" layer of *ca.* 150 μm thickness is made of an ethylene/vinyl alcohol copolymer containing 29% of ethylene (EVOH). The two remaining layers correspond to an "adhesive" bonding of the HDPE to each side of EVOH, and are present to promote adhesion between

HDPE and EVOH, which is not directly thermodynamically favourable. This "adhesive" is based on a linear low-density polyethylene (LLDPE) which has been functionalised by grafting of maleic anhydride (MA), and its thickness is *ca.* 100 μm. Thus, the structure of the five-layer multimaterial is HDPE/PEg/EVOH/PEg/EVOH, and its overall thickness is *ca.* 3 mm. In this study, it is the adhesion at the interface EVOH/PEg which is of interest to us in particular, that at the interface HDPE/PEg being assured by thermodynamic compatibility.

Tensile Tests

Mechanical properties of the individual polymers were assessed using tensile tests in a tensile tester (Instron, Canton, Massachusetts, USA), at a rate of 5 mm·min^{-1}, and in ambient conditions. Dumbbell-shaped specimens of gauge width 4 mm were cut from the coextruded materials. To obtain true stress-strain properties, a small cell of 2 mm in height (by 4 mm in width) was drawn on the specimen surface, and followed by video recording during the test. Longitudinal and tranverse deformations were then deduced from the height and width of the deformed cell. True stress was obtained from the force applied divided by the actual cross-section of the specimen. As may be seen Figure 3, a bilinear representation is a good approximation to the true-stress strain properties of the materials, in the range $\varepsilon < 1$. The parameter α is defined as the ratio of the modulus of the polymer in the second deformation stage to the initial modulus (Figure 3). Young's modulus, E, yield stress, σ_0, and parameter, α, are given in Table 1 for the materials.

Peel Tests

L-peel tests were performed on the five-layer material. One side (HDPE) of the specimen was attached to a backing plate employing a method described elsewhere [9]. Using a blade, a crack was then initiated at the desired PEg/EVOH interface. In the first configuration, L-A, the peeled arm was composed of HDPE/PEg layers (Figure 4). In a second configuration, L-B, the peeled arm was composed of HDPE/PEg/EVOH layers. For both L-peel tests, separation was assured at a constant overall peel angle, θ, using a specific mounting rig, already described in the literature [13]. T-peel tests were also performed on the five-layer material, in which the peel arms, HDPE/PEg/EVOH and HDPE/PEg, were attached to the tensile tester and the unpeeled section was free to orientate to a natural value of θ. Separation was assured at an overall angle of 180°.

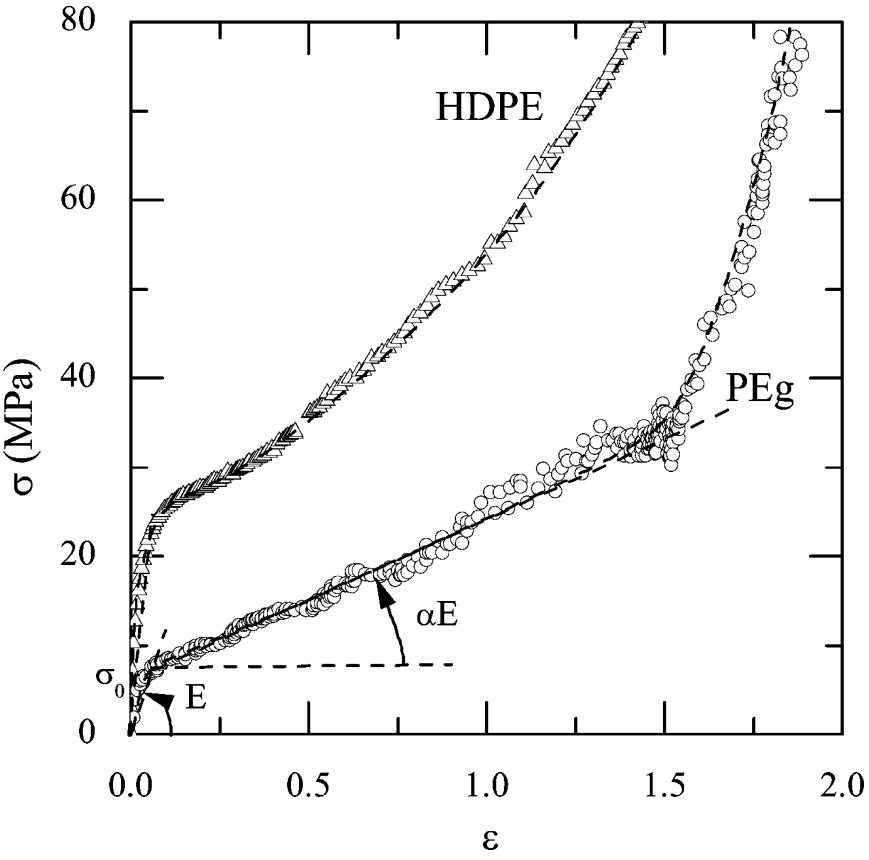

FIGURE 3 Uniaxial tensile true stress-true strain curve for HDPE and PEg, and bilinear representation.

Peel tests were undertaken in a tensile testing machine (Instron) at a nominal speed of separation of 5 mm·min^{-1}, in ambient conditions. The geometry of the specimen was also analyzed from photographs taken during the experiments.

TABLE 1 Mechanical Properties of the Materials

	E (MPa)	σ_0 (MPa)	α
HDPE	700 ± 20	21 ± 0.2	0.04
PEg	170 ± 5	8.0 ± 0.2	0.1
EVOH	3100 ± 100	100 ± 20	—

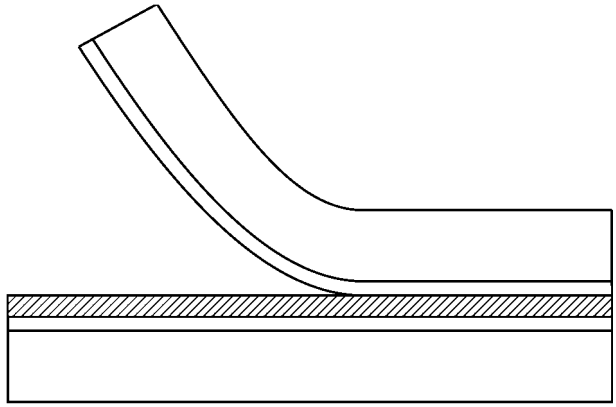

L-peel A

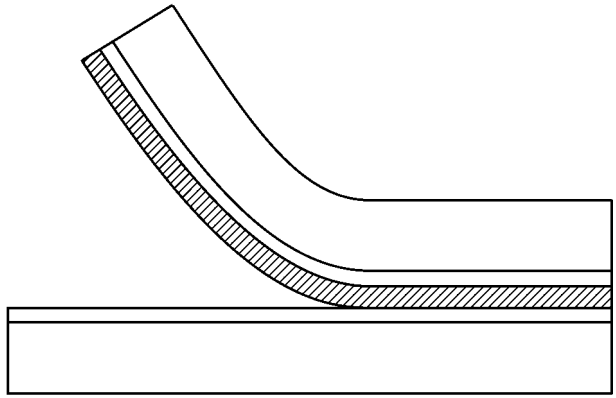

L-peel B

FIGURE 4 Peel geometries L-A, L-B. Specimen is a five-layer material HDPE/PEg/EVOH/PEg/HDPE.

SEM Observations

Scanning electron microscopy (SEM) was used to observe peel front, interphase, and polymer surfaces after peeling. Specimens were observed in SEM (Leo Gemini DSM 982, Cambridge Instruments, Cambridge, UK) at 2 kV or 5 kV after deposit of a 3 nm Au-Pd coating. Different sample preparations were used depending on the specimen.

To observe adhesive deformation at the peel front, the peel sample was embedded in a low viscosity epoxy resin during the test to maintain stress. The sample was then machine cut through a section after curve of the epoxy and the surface gently polished with 1 μm diamond powder. The sample was finally etched with a permanganic method proposed by Basset [31, 32]. This technique leads to slight dissolution of the EVOH surface, but this layer is of no direct interest to us since all deformation occurs on the PEg side. PEg and EVOH surfaces were also observed directly after peeling, with no surface preparation. To observe the interface, a special technique was used to obtain as little deformation as possible in the adhesive during preparation. The five-layer coextruded sample was cleaved rapidly in liquid nitrogen, and the sections, presenting all layers, were observed in the SEM. We have checked that this cryogenic exposure has no significant effect on peel energy of the sample.

RESULTS AND DISCUSSION

Effect of Peel Angle and Geometry

A series of identical specimens was peeled in the various configurations (L-A, L-B, T), and at different peel angles (for L-A and L-B). For each experiment, we took optical photographs of the peel front during peeling, and measured values of radius of curvature, R_0, and opening angle, θ_0. Experimental values may be compared with the theoretical values given by solving Equations (10) and (12) numerically (Figure 5). Satisfactory agreement may be seen, not only for the opening angle, as reported before [13, 30], but also for radii of curvature, given the intrinsic uncertainty of experimental evaluation of both quantities. Similar results have been found for L-peel B tests. Taking the calculated radius of curvature, it is possible to estimate the energy of adhesion, G_A, *via* Equations (3) and (5). Results are shown in Figure 6 for L-peel A and in Figure 7 for L-peel B. The results are similar to those obtained in our previous paper [9], but with much less scatter. For T-peel tests, results are summarized in Table 2, since we have only an angle of 180°.

The satisfactory agreement between calculated and measured values of R_0 and θ_0 substantiates the model that we proposed, even if we are concerned with very high peel energies (~ 10 kJ·m^{-2}). As may be seen in Table 2, close agreement of theoretical values with experimental values are also found for T-peel tests. The application of the model to T-type peel tests seems to be a novelty for the adhesion of thermoplastics.

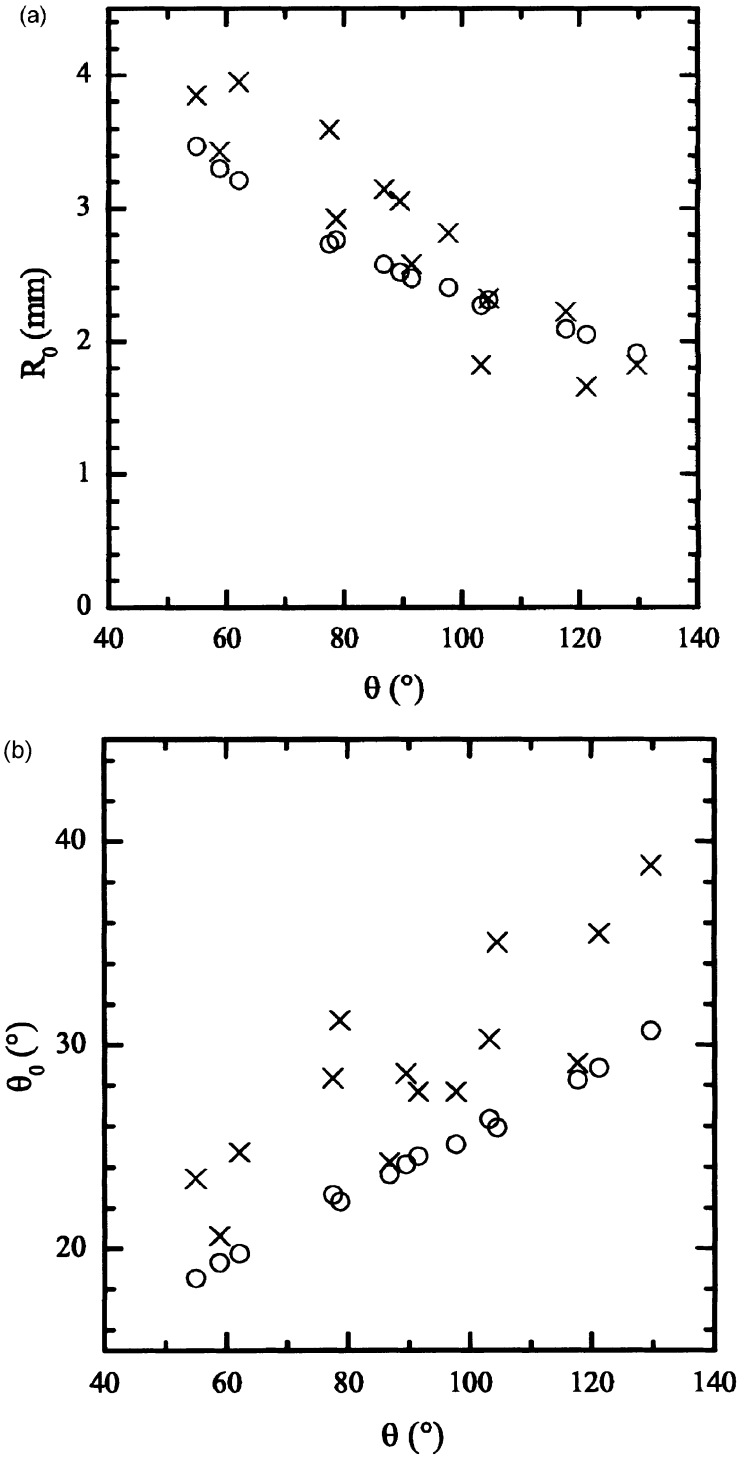

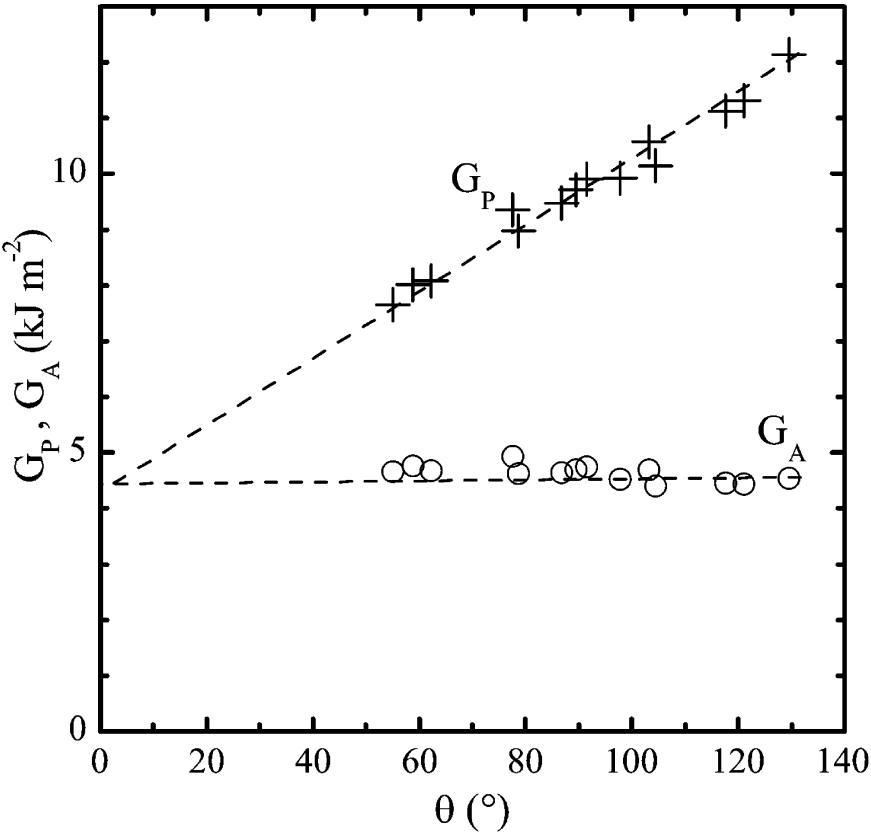

FIGURE 6 L-peel A experiment. Measured peel energy (+), and calculated peel adhesion (◦).

Looking at Figures 6 and 7, it is interesting to note that, when extrapolating data of $G_P(\theta)$ and $G_A(\theta)$, the lines intersect quite close to $\theta = 0$. This may be explained by the idea, proposed by Gent and Kaang [17] that for small angles, thus for small curvatures, the energy dissipated in volume by bending vanishes. This result constitutes supplementary evidence for the value of G_A found.

One may also observe that peel adhesion is little influenced by peel angle, at least for the L-peel A experiment. This result is not trivial

FIGURE 5 L-peel A experiment. Comparison of experimental (×) and theoretical (◦) values of radius of curvaturre (a) and root rotation (b) for different peel angles.

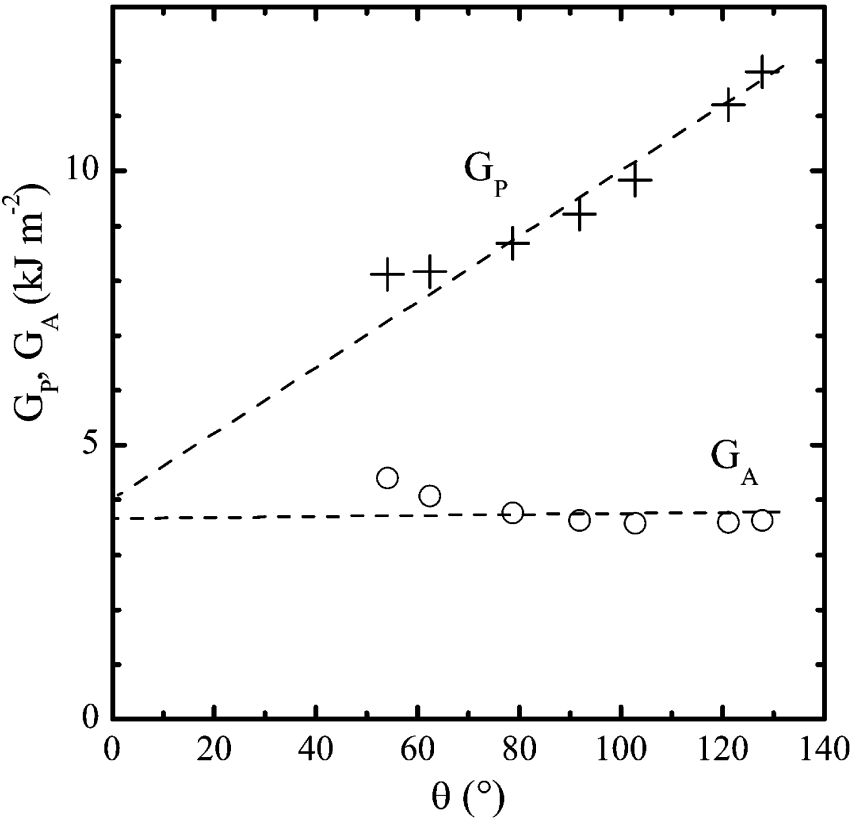

FIGURE 7 L-peel B experiment. Measured peel energy (+), and calculated peel adhesion (◦).

since one might think that the local state of stress and deformation at the crack tip should strongly depend on peel angle. This idea was actually refuted by the finite element analysis of Crocombe and Adams [33] who found that peel angle had little effect on energy of adhesion. Also, to compare the effect of peel geometry on energy of adhesion, we

TABLE 2 T-Peel Test: Comparison Between Experimental and Calculated Geometrical Parameters

	θ_{01} (°)	θ_{02} (°)	R_{01} (mm)	R_{02} (mm)
Experimental	23.5 ± 3	11.2 ± 3	2.9 ± 0.5	8.3 ± 1
Theoretical	19.9	7.8	2.8	7.8

TABLE 3 Comparison of Energy of Adhesion for Three Peel Geometries at a Separation Speed of 5 mm·min^{-1}

	G_P (kJ·m^{-2})	G_A (kJ·m^{-2})
L-peel A, $\theta = 90°$	9.8	4.7
L-peel B, $\theta = 90°$	9.2	3.6
T-peel	8.8	3.1

have summarized in Table 3 the calculated energy of adhesion for the three peel geometries. Further discussion needs information about local stress, which we shall study now.

Craze Structure and Deformation Mechanism

In our earlier paper [9], we showed optical photographs of the crack tip revealing the existence of a plastic deformation zone near the crack tip. A more detailed view of the craze obtained by electron microscopy is given in Figure 8. We observe a clear deformation zone near the crack tip (note that slight relaxation, visible at the crack tip, has occurred during encapsulation). A closer look at the craze structure (Figure 9) reveals that the craze is composed of fibrils elongated in the direction of the maximum stress. From these and other microscopic observations of the same kind, we may give an estimate of the typical critical crack tip opening displacement, $\delta_c = 80 \pm 15\,\mu m$, and of the maximal extension of the fibril at the crack tip of $h_f = 100 \pm 20\,\mu m$. Figure 10 shows the layer of material affected by plastic deformation after relaxation, whose effective thickness is $e_\infty \simeq 10\,\mu m$. In the middle of the craze, fibrils are oriented perpendicularly to the interface, at an angle $\alpha = 0$ with respect to the y axis. After complete relaxation of the craze, Figure 10 shows that the fibrils are oriented at an angle, α_∞, from the interface greater than 90°. The length of the fibrils, $h_{f\infty}$, after relaxation is close to h_f because of the fibrils' angle, which shows that little relaxation has occurred after crack tip.

Figures 11 and 12 show the surfaces of the PEg and EVOH after peeling. We observe on the PEg side a dense network of fibrils of about 50 nm in diameter and a few tens of microns in length. Small quantities of the same fibrils may be seen on the EVOH side. In Figure 13, obtained by fast cleavage of a specimen in liquid nitrogen, we observe the formation of an interphase where small fibrils formed perpendicularly to the interface. It is possible that this interphase has been formed during specimen preparation and, thus, is not a characteristic of the material. However, since we also observe these fibrils during (Figure 9) and after

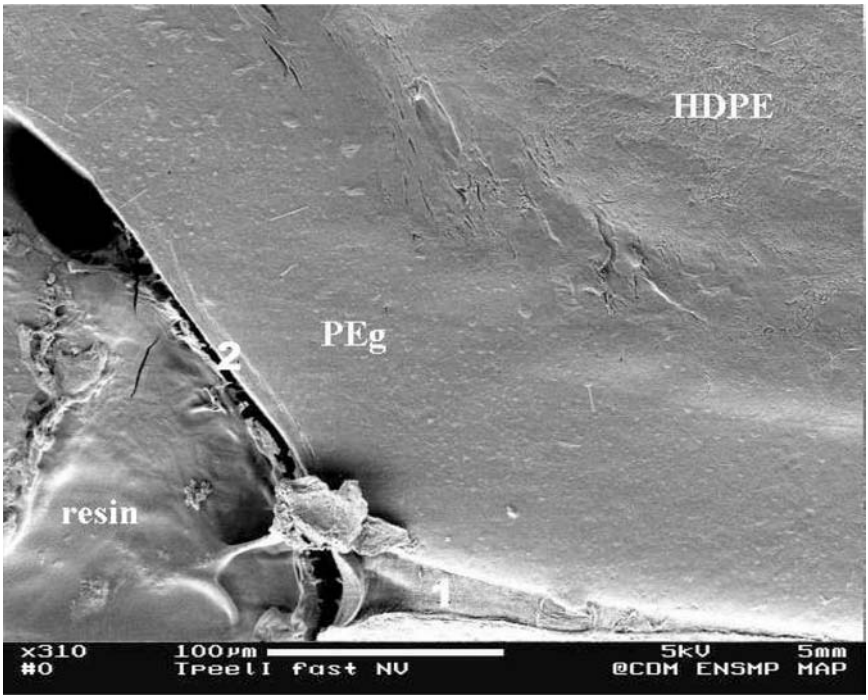

FIGURE 8 Profile of the PEg/EVOH interface under peel load. EVOH surface has been dissolved by an etching process. Craze domain is designated by 1. Scale : bar = 100 μm.

(Figure 11) craze formation, we believe that the formation of the fibrils is the first deformation mechanism to occur at the interface under fracture stress. The second step in the deformation mechanism is the growing of the craze structure by fibril elongation. This process has been previously described for amorphous and semicrystalline polymers. The fibrils draw fresh material from the craze/bulk interface to grow. Since this occurs only on one side of the craze, the fibrils are not supplied with material from the EVOH side. Their cross-section decreases, and the fibrils eventually break close to the EVOH side by chain scission and/or disentanglement. However, chain disentanglement is less probable since high stresses are involved.

Estimation of the Local Energy Dissipation

If we consider the deformation zone of Figure 8 as a Dugdale zone, we may estimate the energy dissipated in the formation of the zone from

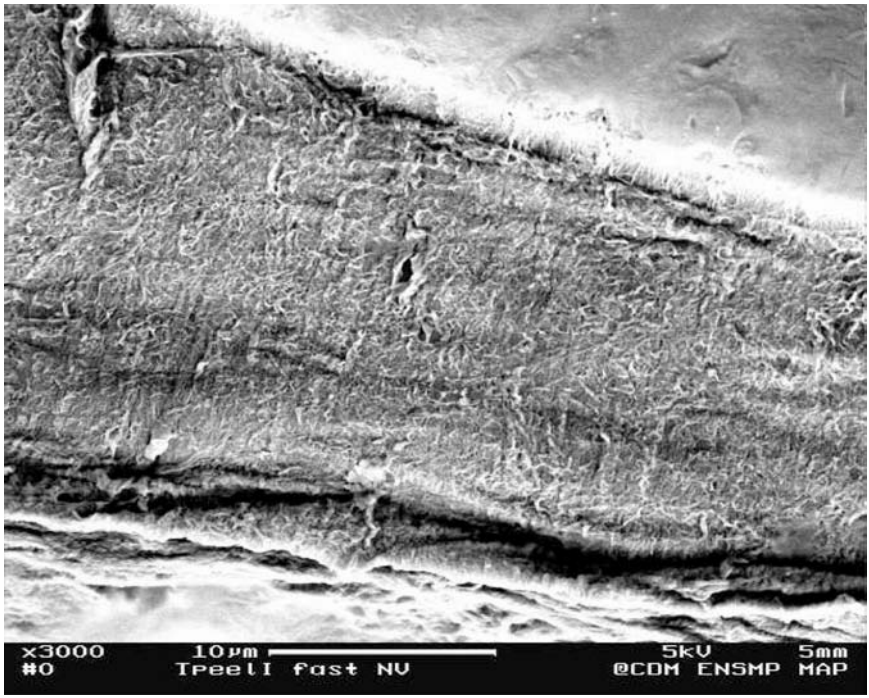

FIGURE 9 Enlargement of domain 1 in Figure 8. Scale : bar = 10 µm.

$G = \sigma_0 \delta_c$. Experimentally, δ_c has been found to be about 80 µm. From microscopic observations, we find the displacement of the PEg layer at the crack tip to be $y(0)_{\mathrm{PEg}} \simeq 100\,\mu\mathrm{m}$. Thus, the global strain of the PEg layer at the crack tip is $\varepsilon_{\mathrm{PEg}} = y(0)_{\mathrm{PEg}}/h_a \simeq 1 \pm 0.2$, with h_a the nominal thickness of the PEg layer at the crack tip. If we consider this value on the true stress-true strain (natural logarithm of current length divided by initial length) curve for PEg (Figure 3), we find a stress at the crack tip of about 25 MPa. The deformation of the HDPE at this stress value from the stress-strain curve is $\varepsilon_{\mathrm{HDPE}} \simeq 0.06$, corresponding to a displacement of the HDPE layer $y(0)_{\mathrm{HDPE}} \simeq 75\,\mu\mathrm{m}$. Finally, the global displacement of the beam at the crack tip is $y(0) = y(0)_{\mathrm{HDPE}} + y(0)_{\mathrm{PEg}} \simeq 175\,\mu\mathrm{m}$. We may calculate the theoretical displacement of the beam from the beam on an elastic foundation model *via* Equation (11), which yields $y(0) = 165\,\mu\mathrm{m}$ for $(\theta - \theta_0) = 0$ up to 195 µm for $(\theta - \theta_0) = 90^\circ$, which corresponds well with the measured displacement.

Taking values of 25 MPa for σ_0 and 80 µm for δ_c, we then have an adhesion energy estimated from the Dugdale model of

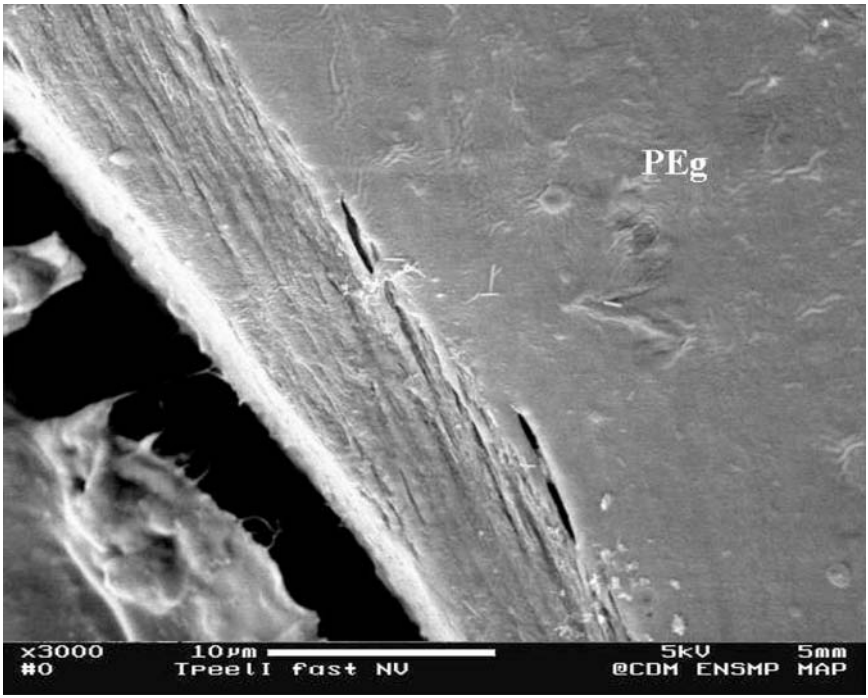

FIGURE 10 Enlargement of domain 2 in Figure 8. Scale: bar = 10 μm.

$G = \sigma_0 \delta_c \sim 2\,\mathrm{kJ \cdot m^{-2}}$. This is about half the estimated values of G_A in Table 3. There are at least two other possible sources of energy dissipation which may explain the discrepancy. As observed in other semicrystalline systems, there may be some other diffuse zones of plastic deformation at large distances from the interface. This is obvious at high peel speeds, as shown in our recent paper [9] but taking into account the high peel energies, some other deformation processes may occur even at low speeds, although they are not visible with optical or electronic microscopy. Also because, of the subjacent network of fibrils that appears in Figure 11, fibrils may transmit stresses to their neighbours. Important stresses may then be found between crack faces for some distance after the Dugdale zone, in the region $x < 0$. The Dugdale model does not take into account any energy dissipation in this region, although we believe that it may be a significant contribution to the apparent energy. To illustrate this assertion, we shall study the consequence of reorientation of the fibrils after the crack tip.

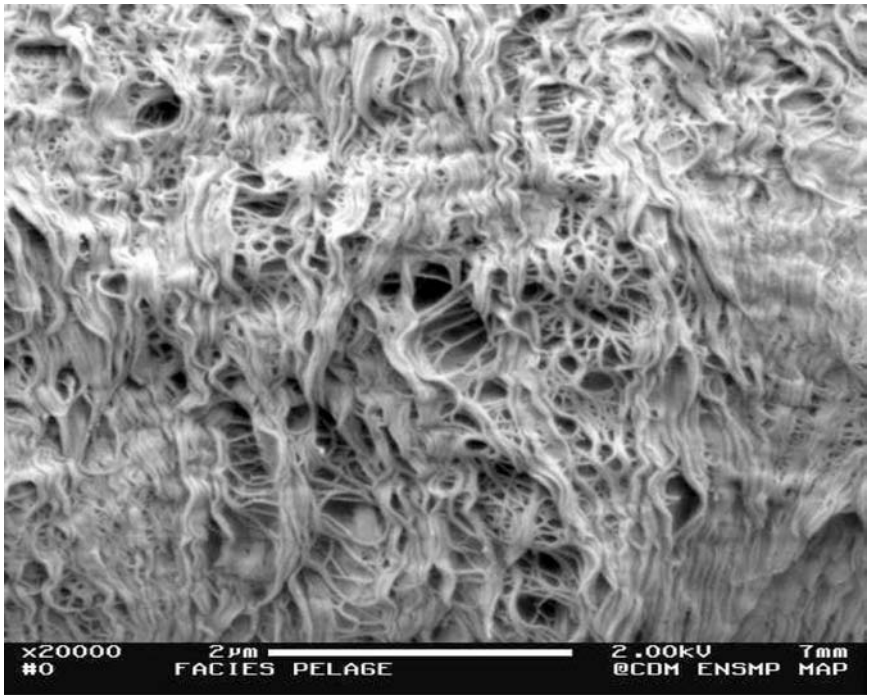

FIGURE 11 PEg surface after L-peel A. Peel direction is downward. Scale: bar = 2 µm.

Reorientation of the fibrils is due to some shear stress, τ_0, in the region $x < 0$ (Figure 14). Simplifying into the two regimes—tension σ_0 for $x > 0$ and shear τ_0 for $x < 0$—we attempt to estimate the latter contribution. Kaelble [14] analysed shear stresses in a peel test and showed that shear stresses within an adhesive layer may be expressed as [14, 16]:

$$\tau(x) = \frac{F\cos\phi}{b}\lambda_T e^{-\lambda_T x}; x \geq 0, \tag{13}$$

where

$$\lambda_T = \left(\frac{\mu_a}{Ehh_a}\right)^{1/2}, \tag{14}$$

μ_a represents the shear modulus of the "adhesive" layer (PEg), and ϕ is the local peel angle near the crack front. Clearly, in the purely elastic case, we have

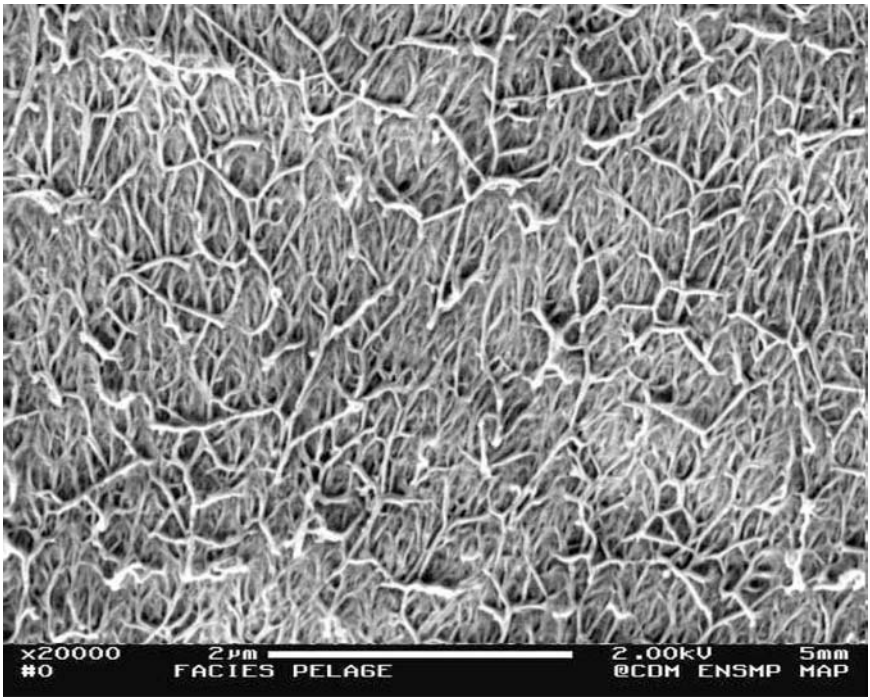

FIGURE 12 EVOH surface after L-peel A. Peel direction is downward. Scale: bar = 2 µm.

$$\tau_0 \simeq \tau(0) = \frac{F \cos \phi}{b} \lambda_T \tag{15}$$

with an exponential decay as x increases. An abrupt cut-off is assumed for $x < 0$, but our observation has shown the effect of shear in this region for the system studied. A rigorous analysis of shear for $x < 0$ has not been undertaken (and, we suggest, may well be complex!), but we tentatively propose that shear stress along the HDPE/PEg interface will remain essentially constant, corresponding to a plastic reorientation of the PEg, while the angle of orientation of the craze structure, α, (Figure 14) evolves from *ca.* 0 to its final value, α_f. No significant further extension of the fibrillar zone beyond δ_c is taken into account. Thus, following the Dugdale scheme, and ignoring a prefactor which may well be difficult to evaluate (being related to the decay of $\tau(x)$ for $x < 0$), we may define a shear contribution to effective fracture energy:

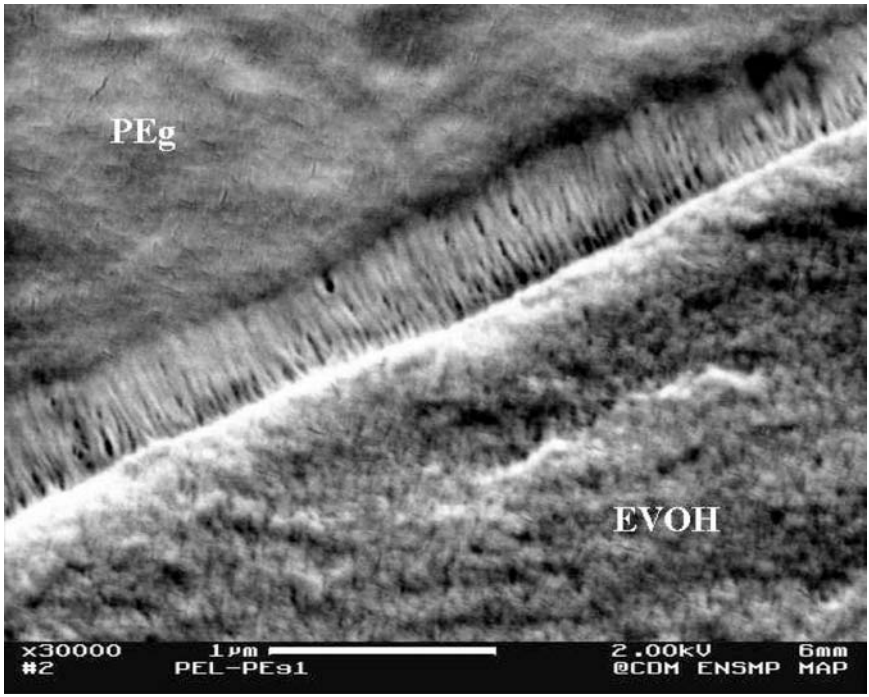

FIGURE 13 Interphase between PEg and EVOH. Scale : bar = 1 μm.

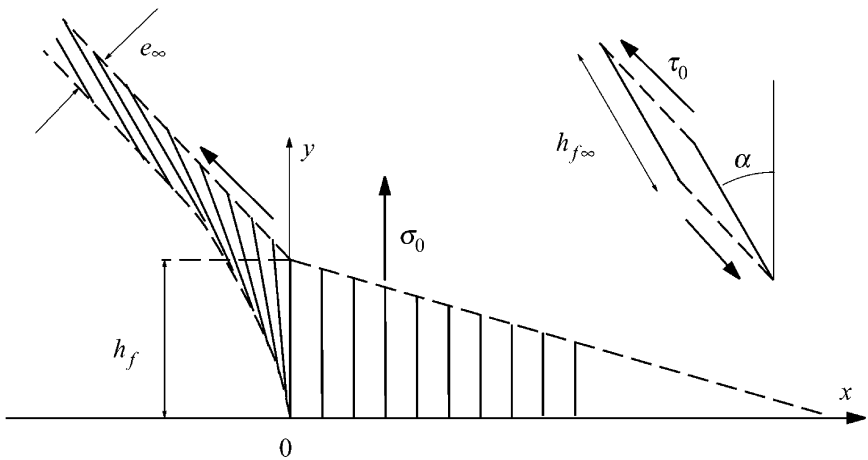

FIGURE 14 Schematic of deformation of PEg near peel front. For $x > 0$, deformation is principally in tension; for $x < 0$, principally in shear.

$$G_A^S = \int_0^{\alpha_f} \tau(x)\delta_c \mathrm{d}(\sin\alpha) \simeq \int_0^{\alpha_f} \tau_0\delta_c \mathrm{d}(\sin\alpha) \simeq \frac{P\cos\phi}{b}\lambda_T\delta_c. \qquad (16)$$

With $\mu_a = 60\,\mathrm{MPa}$, $\lambda_T = 0.8\cdot\mathrm{mm}^{-1}, \phi = \pi/4, \delta_c = 80\,\mu\mathrm{m}$, we obtain $G_A^S \sim 0.5\,\mathrm{kJ}\cdot\mathrm{m}^{-2}$. Clearly, simplifications have been adopted in calculating G_A^S, but this result shows that the effect of reorientation of the fibrils after the Dugdale zone may be a significant contribution to the dissipated local energy.

CONCLUSION

A study of the adhesion of two semicrystalline polymers, HDPE and EVOH, bonded by a grafted LLDPE "adhesive" (PEg), has been undertaken using three peel geometries. The interface of interest, at which failure occurs, was that of PEg/EVOH. The system studied corresponds to a five-layer system: HDPE/PEg/EVOH/PEg/HDPE. Two peel tests, denoted L-peel A and L-peel B, involve, respectively, peeling a free arm of HDPE/PEg and HDPE/PEg/EVOH from the remaining constituents attached to a fixed backing. The remaining, T-peel test, represents a 180° geometry in which both arms are free. It was shown that the overall, measured, peel energy for L-peel increased with peel angle. Results have been analysed, taking into account bending arm curvature and opening angle at the advancing crack tip, or peel front. The model used is based on elastic foundation theory for the unpeeled component and global elastoplastic analysis for the peeled arm. Good agreement was obtained between experimental measurements of peel curvature and opening angles, and values obtained from theoretical analysis. The model was extended to T-peel, and satisfactory correlation was also obtained between experiment and theory. Following from the analysis, it was possible to show that once bulk energy dissipation due to bending of the peel arm(s) had been taken into account, the remaining adhesion energy expenditure, which may be associated with local interfacial failure and craze formation, was remarkably independent of peel angle, suggesting that the same separation mechanisms are involved at a local scale. However, the calculated value of adhesion energy is somewhat larger than that expected from the Dugdale model. SEM examination revealed the presence of a plastic deformation region in the PEg near the crack front, in agreement with stress calculations. This region was composed of small fibrils that had apparently formed very early to create an interface of about 1 μm. SEM evidence suggests that the fibrils then grow in a direction perpendicular to the interface, as in a

craze growth mechanism, change their orientation at the crack tip, and eventually break near the EVOH side. A rough estimate of the energy dissipated in this change in fibril orientation shows that it may significantly contribute to the fracture energy. This preliminary study points to the fact that some energy dissipation and, therefore, increased fracture toughness may be associated with a mode of polymer deformation in which cavitation, and thus volume change, is not implicit.

REFERENCES

[1] Kausch, H. H., and Tirrell, M., *Ann. Rev. Mater. Sci.*, **19**, 341–377 (1989).
[2] Wool, R. P., Yuan, B. L., and Mac Garel, O. J., *Polym. Eng. Sci.*, **29**, 1340–1367 (1989).
[3] Gent, A. N., and Hamed, G. R., *J. Adhesion.*, **7**, 92–95 (1975).
[4] Levine, M., Ilkka, G., and Weiss, P., *J. Polym. Sci., Polym. Phys.*, **B2**, 215 (1964).
[5] Gent, A. N., and Petrich, R. P., *Proc. Roy. Soc. A*, **310**, 433–448 (1969).
[6] Gent, A. N., and Hamed, G. R., *J. Applied Polymer Science.*, **21**, 2817–2831 (1977).
[7] Gent, A. N., and Jeong, J., *Int. J. Fracture.*, **29**, 157–158 (1985).
[8] Mantel, M., and Descave, F., *J. Adhesion Sci. Technol.*, **6(3)**, 357–376 (1992).
[9] Guiu A., and Shanahan, M. E. R., *J. Polym. Sci. B: Polym. Phys.*, **39**, 2843–2851 (2001).
[10] Kim, K.-S., and Aravas, N., *Int. J. Sol. Struct.*, **24**, 417–435 (1998).
[11] Aravas, N., Kim, K.-S., and Loukis, M. J., *Mat. Sci. Eng.*, **A107**, 159–168 (1989).
[12] Williams, J. G., *J. Adhesion.*, **41**, 225 (1993).
[13] Kinloch, A. J., Lau, C. C., and Williams, J. G., *Int. J. Fracture.*, **66**, 45–70 (1994).
[14] Kaeble, D. H., *Trans. Soc. Rheol.*, **IV**, 45–73 (1960).
[15] Kanninen, M. F., *Int. J. Fracture*, **9**, 83 (1973).
[16] Maugis, D., *Contact, adhesion and rupture of elastic solids* (Springer, Berlin, 2000).
[17] Creton, C., Kramer, E. J., Hui, C. Y., and Brown, H. R., *Macromolecules*, **25**, 3075–3088 (1992).
[18] Washiyama, J., Creton, C., and Kramer, E. J., *Macromolecules*, **25**, 4751–4758 (1992).
[19] Plummer, C. J. G., Kausch, H.-H., Creton, C., Kalb, F., and Léger, L., *Macromolecules*, **31**, 6164–6176 (1998).
[20] Dugdale, D. S., *J. Mech. Phys. Solids*, **8**, 100–104 (1960).
[21] Brown, H. R., *Macromolecules*, **24**, 2752–2756 (1991).
[22] Döll, W., In: *Adv. Polym. Sci.*, vol. 52/53, Kausch, H. H., Ed. (Springer, Berlin, 1983).
[23] Kalb, F., Léger, L., Creton, C., Plummer, C. J. G., Marcus, P., and Magalhaes, A., *Macromolecules*, **34**, 2702–2709 (2001).
[24] Brown, H. R., and Ward, I. M., *Polymer*, **14**, 469–475 (1973).
[25] Moidu, A. K., Sinclair, A. N., and Spelt, J. K., *J. Testing Evaluation*, **26**, 247–254 (1998).
[26] Kendall, K., *J. Phys. D: Appl. Phys.*, **8**, 1449–1452 (1975).
[27] Gent, A. N., and Kaang, S. Y., *J. Adhesion*, **24**, 173–181 (1987).
[28] Winkler, E., *Die Lehre von der Elastizität und Festigkeit* (Prague, 1867).
[29] Penado, F. E., *J. Comp. Mat.*, **27**, 383–407 (1993).

[30] Moore, D. J., and Williams, J. G. In: *Fracture of polymers, composites and adhesives*, Williams, J. G., and Pavon, A., Eds., vol. 27 (Elsevier, Amsterdam, 2000).
[31] Basset, D. C., and Hodge, A. M., *Proc. Roy. Soc. London*, **A377**, 25–37 (1981).
[32] Olley, R. H., and Bassett, D. C., *Polymer*, **23**, 1707–1710 (1982).
[33] Crocombe, A. D., and Adams, R. D., *J. Adhesion*, **12**, 127–139 (1981).